5 #1

ELECTRONIC PROGRESS

RAYTHEON

HILL LIBRARY
AUG 30 1960
North

JULY-AUGUST 1960

in this issue:

The AMPLITRON

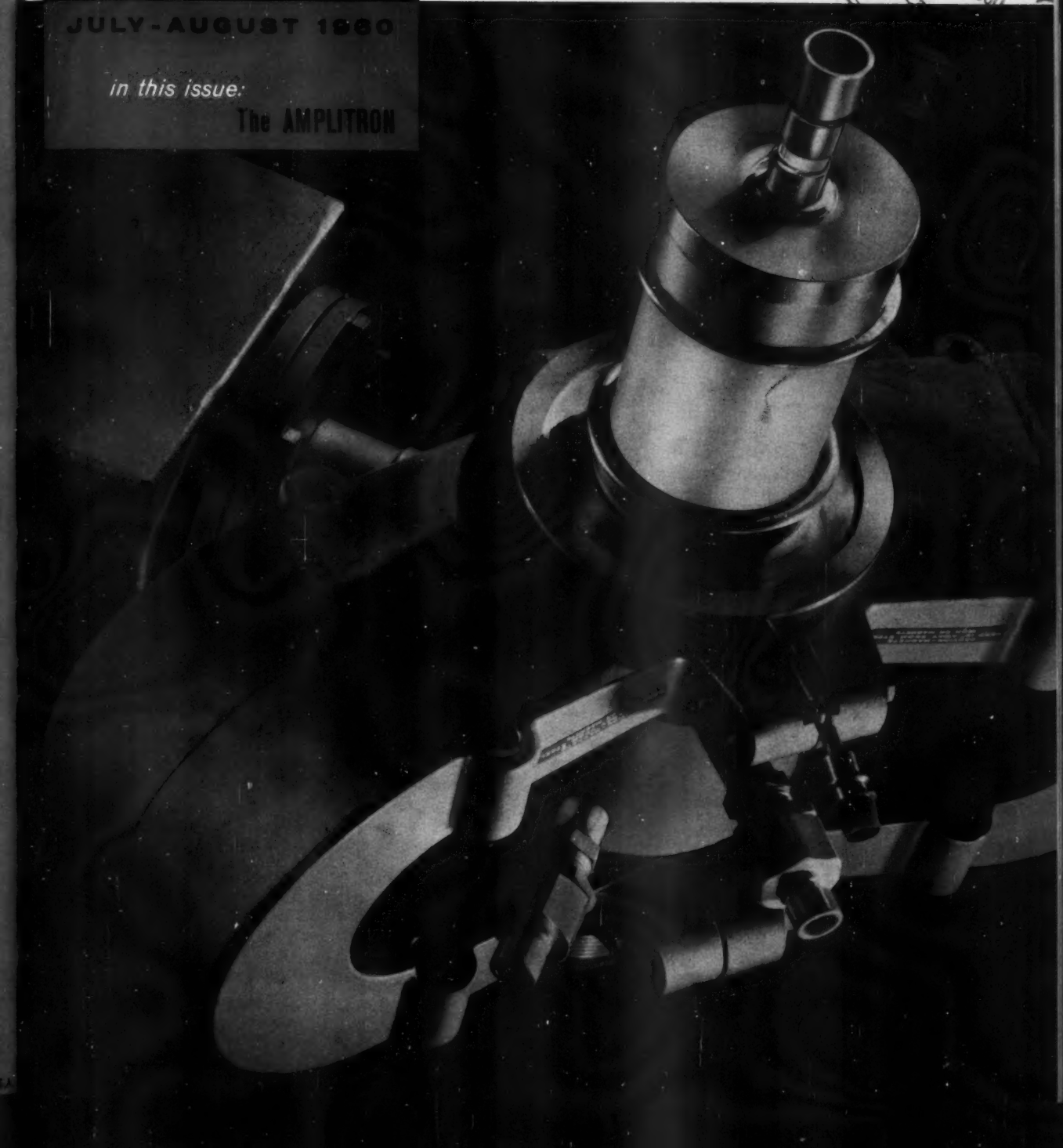

VOLUME V JULY-AUGUST 1960 NUMBER 1

ELECTRONIC PROGRESS

Copyright 1960, Raytheon Company, Waltham 54, Mass.

RAYTHEON

1 The Amplitron — A Super Power Microwave Generator — *William C. Brown*

5 Papers and Publications

6 Direct Solar Power Conversion for Space Vehicles — *Richard C. Barbera, David L. Dayton*

12 Stabilization — *Richard E. Lang*

EXECUTIVE EDITOR *Ivan A. Getting* • **MANAGING EDITOR** *Michael A. Walker* • **EDITOR** *Frances Dal Corobbo* • **ART EDITOR** *William Niles*

Printed in U.S.A.

EDITORIAL ADVISORY BOARD

Lawrence Batchelder
Submarine Signal Operations

Thomas Cutler
Missile Systems Division

Robert Edwards
Microwave and Power Tube Division

Peter Fowler
Industrial Components Division

John Harmer
Airborne Electronic Equipment Operations

Melvin Holland
Research Division

John Meade
Surface Radar and Navigation Operations

Gordon Partridge
Communications and Data Processing Operations

William Root, Jr.
Commercial Apparatus and Systems Division

John Shea
Semiconductor Division

Vergil Wall
Santa Barbara Operations

THE COVER

Our cover photo shows Raytheon's first Amplitron to be used for non-military applications, the QK653. This tube is employed in FAA air traffic control radars built by Raytheon; over 30 such systems will be in operation by the end of 1961. The sophisticated performance of the QK653 is one of the reasons for the interest in super power Amplitrons, as discussed in this issue's feature article.

THE AMPLITRON

a super power microwave generator

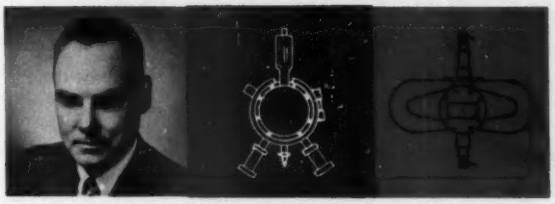

WILLIAM C. BROWN *is Associate Director of Engineering, Crossed-Field Devices, Microwave and Power Tube Division. For the past fifteen years he has been active in microwave tube design and development and is responsible for a number of advances in crossed-field devices, including the platinotron and its Amplitron and Stabilotron derivatives. Mr. Brown holds B.S. and M.S. degrees in Electrical Engineering from Iowa State College and MIT, respectively. He is a Fellow of the IRE.*

ONE of the most exciting new developments in electronics is the possibility of generating economically with a single tube very large amounts of microwave power. Such power levels will be measured in the hundreds of horsepower at wavelengths of ten centimeters or less from a single tube. This development will make possible radars of greatly increased range and sophistication. A far more intriguing implication of the availability of large amounts of economically generated power is a completely new direction of growth of the electronics industry — the transfer of power from one point to another by electromagnetic beams.

The ability to generate large amounts of power in a single envelope has the additional attraction of reducing the cost of microwave tubes on a "per kilowatt basis." Such a reduction in tube cost and the accompanying reduction in amortization costs over the life of the tube, coupled with the inherently high efficiency of these devices, may make possible new applications for microwave tubes in the highly competitive heat processing area.

The intent of this paper is to emphasize the engineering considerations involved in the power aspects of a super power tube development, however, the actual selection of a class of tube for super power development may depend upon many other requirements of the intended applications for such tubes. Although applications for super power tubes vary in their requirements, a high percentage require sophisticated performance characteristics such as broad electronic bandwidth, linearity of phase change through the device as a function of frequency, and insensitivity of phase output to external influence. The Amplitron with its demonstrated performance as a device possessing these characteristics, coupled with very high efficiency and simple mechanical construction, has made it a logical choice for investigation as a super power device.

Additional insight into the nature of the requirements for a super power development may be obtained from a historical review of the progress which has been made in the generation of microwave power. Figure 1 shows the progress that has been made in average power generation at S band (10 cm) from 1938, when microwave tubes were first introduced, to the present. By 1950 the magnetron had been developed to about 5 kw of average power output, and progress had been at the rate of a tenfold increase every five years. If that rate of progress had been maintained, power levels of the order of 500 kilowatts would now be available. In 1950, however, the requirements for radar equipment, which had been the motivating influence for higher power tubes, changed to a more sophisticated type of operation requiring an amplifier type of transmitting tube. In the development of microwave tubes after 1950, emphasis was placed on development of amplifying types of tubes even though this meant a temporary slow-down in the development of average RF power. Recognizing this change of emphasis, the Raytheon Company introduced the Amplitron device in 1955. The Amplitron retained the high efficiency and simple mechanical construction of the magnetron oscillator while introducing amplification over a broad band of frequencies with negligible phase distortion and a number of other desirable

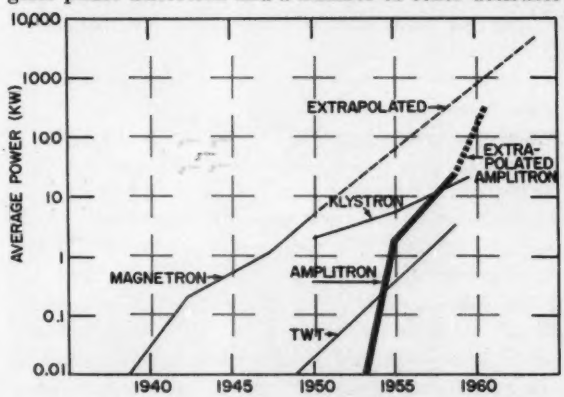

Figure 1. Progress in Power Generation vs. Time for Microwave Tubes at S-Band

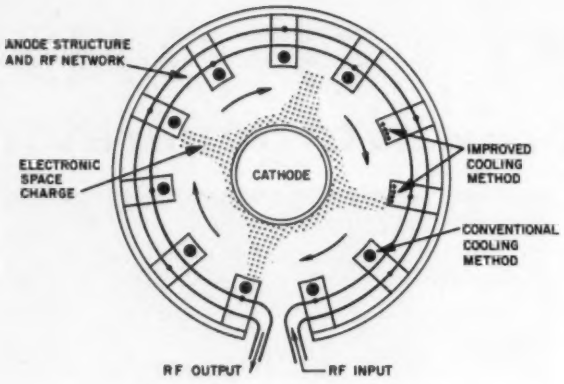

Figure 2. Schematic Diagram of Amplitron

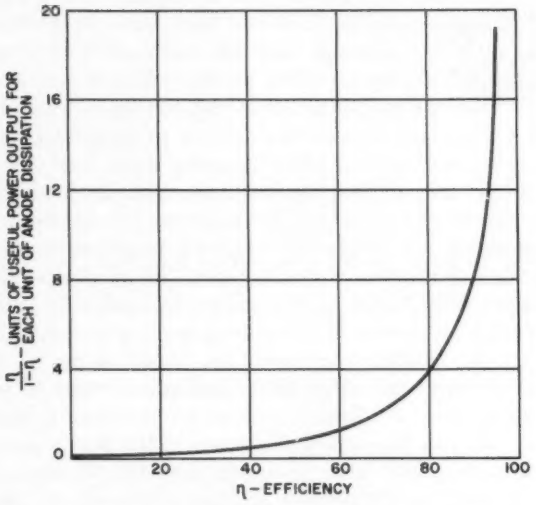

Figure 3. Useful RF Output Power vs. Anode Efficiency

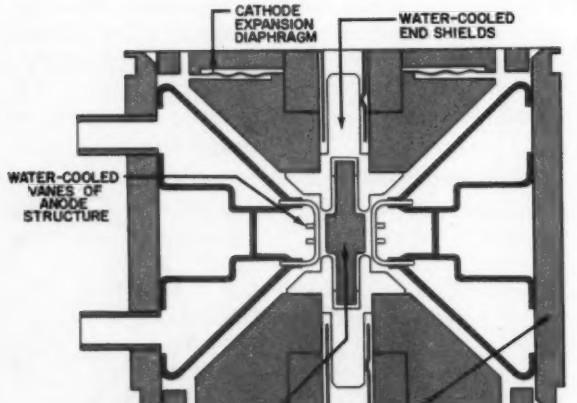

Figure 4. Schematic of X-Band Amplitron

performance characteristics. These characteristics prompted hardware developments for a number of medium power and high power applications. The progress in obtaining average power from the Amplitron was so great that by 1958 a 15-kilowatt average-power S-band tube (QK622) had been developed. This very rapid growth of power from the Amplitron was an additional stimulus for investigating its ultimate power handling potential.

The resulting investigation, begun in 1958, inevitably led to the establishment of the factors which limited the power-handling capability of the Amplitron. These limitations may be better understood by a consideration of how the Amplitron operates. As shown in Figure 2, the Amplitron basically consists of a cathode surrounded by an anode structure and a magnetic field whose direction is normal to the plane of the illustration. The anode structure serves both as a means for carrying the RF wave and as a collecting surface for the electrons emitted from the cathode. To place an Amplitron in operation, a potential is placed between the cathode and the anode. As the potential between cathode and anode is raised, electrons are emitted from the cathode and rotate in concentric orbits about the cathode. As the potential is further increased, the electrons revolve with increasing angular velocity until they become synchronous with the phase velocity of the RF wave on the anode structure. At this point interaction between the electrons and the RF wave occurs, and the electrons coalesce into spokes of space charge which then induce RF currents in the anode structure. These several RF currents induced by the rotating space charge spokes travel in both directions along the RF structure, but tend to add in phase in the direction of the output while canceling in the direction of the input. The interaction mechanism is controlled by the RF introduced at the input terminals of the device so that the output frequency is identical to the driving frequency.

From an energy conversion point of view, the electron has a maximum of potential energy at the cathode surface. As it moves toward the anode, it loses its potential energy and converts from 80 to 90 per cent of this loss directly into useful RF energy. The remaining 10 to 20 per cent is converted into kinetic energy of motion which in turn is converted into heat as the electrons strike and are collected by the anode. It is evident that an increase in efficiency in the operation of the device will decrease the dissipation at the anode and therefore permit more DC power input with correspondingly more RF power output. Further, if the heat dissipation capabilities of the anode surface could be improved, greater power-handling capability would result. Finally, we note that making the RF circuit larger will permit more

anode dissipation and therefore more power input.

It is possible to derive a simple formula in which the RF power output is given as a function of the efficiency and anode dissipation. Such a formula follows;

$$\text{RF Power Output} = [\text{Anode Dissipation}]\,[\text{Efficiency factor}], \quad (1)$$

$$= [(\text{Anode Area})\,(\text{Dissipation Density})]\,[\text{Efficiency Factor}], \quad (2)$$

$$= \left[\left(\frac{K}{f^2}\right)(\rho)\right]\left[\frac{\eta}{1-\eta}\right], \quad (3)$$

where ρ = dissipation density (kw/sq cm)

η = conversion efficiency of DC to RF power

f = frequency of operation

K = constant containing number of vanes, operating potential level, etc.

It will be noted that the RF power output is highly dependent upon efficiency. A plot of the efficiency function $\eta/(1-\eta)$ is given in Figure 3. This efficiency function is identical with the ratio of RF power output to RF power dissipated at the anode. It follows that if the RF power dissipated is a fixed quantity, the RF power output is directly proportional to this function. At 50 per cent efficiency this ratio is unity, at 80 per cent it is four, and at 90 per cent it is nine. A substantial experimental and analytical program is underway at Raytheon to maximize the efficiency of operation of the tube. Such efficient operation of Amplitrons has been obtained that only about 10 per cent of the power input is dissipated in the form of electron bombardment of the anode, corresponding to a conversion efficiency of DC into RF power of 90 per cent. This conversion efficiency corresponds to an observed over-all operating efficiency of as much as 81 per cent in the QK622. The difference between the over-all and conversion efficiency in the tube is accounted for by losses in both the RF circuit and electronic back bombardment of the cathode.

Consider now the problem of achieving a greater dissipation-density capability of the anode. As shown in Figure 2, the conventional cooling technique for an Amplitron is to circulate cooling fluid through a large diameter channel near the face of the vane. From previous work, it was expected that a more efficient form of cooling which would lead to much higher dissipation densities could be derived from the use of a number of small diameter cooling channels rather than one large one, as shown on two of the vanes of Figure 2. To verify this supposition, an X-band tube was constructed. A cross-section of this tube is shown in Figure 4. In this tube the anode structure which collects the electrons is composed of a number of small diameter tubes (0.030 in. O.D., 0.018 in. I.D.) all water cooled in parallel from an inlet and an outlet cooling header. From the anode of this tube, average dissipation densities of as much as 7 kw per sq cm were obtained without destruction of the anode. This value is about twenty times larger than that obtained from cooling designs currently used in microwave tubes.

Because these much higher dissipation densities are obtained with the use of higher pressure cooling systems, it might be concluded that an exorbitant amount of pumping power would be required. In practice, however, a high bulk temperature rise of the coolant is obtained in contrast to systems commonly employed on microwave tubes in which the temperature rise of the coolant is relatively low. The large bulk temperature rise of the high pressure system requires a proportionately smaller amount of volume flow and thus compensates for the higher pressure. The pressure employed may range from 150 to 300 pounds for most applications to as high as 1500 pounds for some special applications. Pumping power requirements can generally be held to about 5 per cent of the DC power supply input to the Amplitron tube itself. Long life pumps for any reasonable pumping pressure and volume flow are readily available. A closed type of cooling system is employed because of the necessity for filtering out fine particles and for maintaining a deoxidized and demineralized state of the water coolant.

It is interesting to examine the effect upon a current Amplitron design of such high density cooling systems as described above. Although the experimentally obtained dissipation density of 7 kw per sq cm could not be considered a conservative design figure at the present time, a density of 3 kw per sq cm could be so considered. If such a dissipation density were applied to the QK622 Amplitron which has an anode area of 22 sq cm, and if the DC to RF conversion efficiency of over 80 per cent in the QK622 is retained, average power outputs of over 200 kw can be expected. This computation is easily demonstrated with the aid of Equation (2).

It is interesting to show the tremendous combined leverage of high efficiency and high anode dissipation density upon power output by plotting contours of values of generated RF power as a function of these two parameters. This is done with the aid of Figure 5. When the high dissipation-density figure of 7 kw is combined with the high electronic efficiency of 90 per cent, both of which have been achieved as maximum experimental values, it will be noted that approximately 70 kw of RF power could be generated for each sq cm of anode area. Although such values

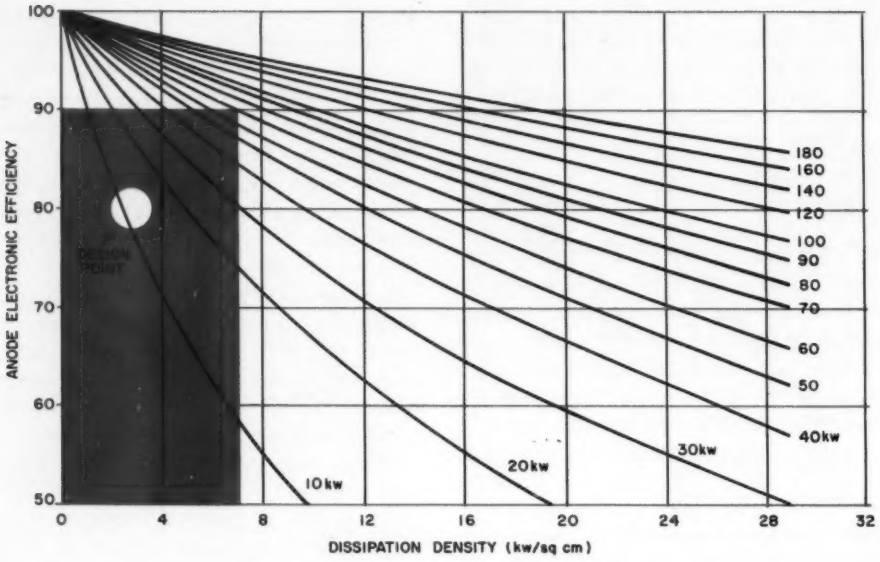

Figure 5. Generated RF Power vs. Anode Area

may be possible at some time in the future, a value of 12 kw per sq cm is currently being used for design purposes.

It is interesting to compare the very high power conversion densities made possible by even this comparatively conservative value of 12 kilowatts per sq cm with those commonly used in other energy conversion processes. For example, in a 4- x 4-inch automobile cylinder about 50 horsepower (37 kw) may be obtained. At a suitable microwave frequency an anode structure of this size could convert 2000 kilowatts of DC power into a nearly equal amount of RF energy.

The generation of large amounts of power from single envelopes, which are both compact and economical to manufacture, has a far-reaching economic significance. Figure 6 shows a proposed 200 kw generator. This is not much larger nor greatly more complicated in construction than the present QK622 which generates about 15 kw of power. Such considerations when combined with production cost figures for fixed frequency magnetrons provide a curve like that of Figure 7. These magnetrons have been in volume production for several years and are quite comparable in their mechanical construction to Amplitrons. This curve indicates that we may eventually obtain large microwave tubes at a cost of about $10 to $20 on a "per kilowatt" basis.

It is of interest to compare this assumed cost with the cost of installation of primary electrical power which runs about $150 per kilowatt of installed capacity in a steam generator plant to $250 per kilowatt in a hydroelectric plant. Power supply rectifier and switch gear would be expected to cost about $100 per kilowatt of installed capacity. It is therefore possible to conclude that in future systems which involve large quantities of microwave power, the microwave tube will not be the limiting factor from an initial cost point of view.

A similar situation with respect to operating costs may be expected. If the microwave tube has a life of 1000 hours and its initial cost is $10 per kilowatt, the amortization cost would be 1 cent per kilowatt hour. This would compare to today's best amortization costs on microwave tubes of 10 cents per kilowatt hour. If such low amortization costs are obtained, it may be expected that microwave energy will find many more uses in areas where it is currently prohibitive from a cost point of view.

In summary, it may be stated that a breakthrough in the generation of large amounts of power from a single envelope is in progress. This breakthrough has come about through the recognition that the high efficiency of the Amplitron and a high anode-dissipation-density cooling system may be combined to permit high-density conversion of DC to RF energy. Because of this, unexpectedly large amounts of power can be obtained from RF generators which scale to relatively small size at microwave frequencies. It should also be noted that the Amplitron device at super power levels retains its desirable properties of broad electronic bandwidth, high efficiency, and simple mechanical construction. This latter property makes it possible to provide power at low cost on a "per kilowatt" basis, so that many applications for microwave devices will no longer be excluded on an economic basis.

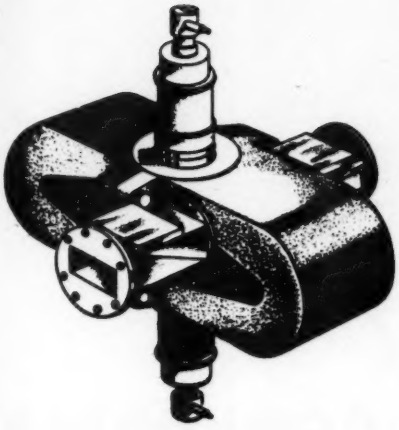

Figure 6. S-Band Amplitron for Operation in 100-200 kw CW Range

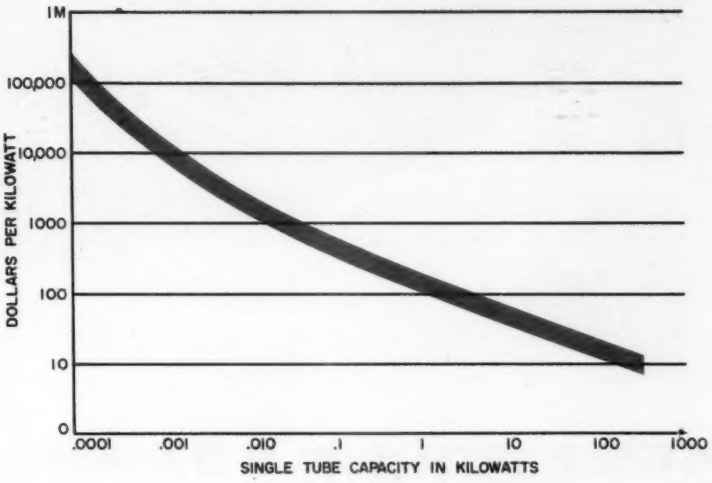

Figure 7. Variation in Cost per Kilowatt of Microwave Power

PAPERS & PUBLICATIONS

W. J. HAYWOOD, JR., "Application of Optical Techniques to Interplanetary Navigation," presented at the Institute of Aeronautical Sciences National Specialists Meeting on Guidance of Aerospace Vehicles, Boston, Mass., May 25, 1960.

This paper presents a method of measuring the relative velocity of an interplanetary vehicle with respect to planets and the sun. Use is made of the fact that the sodium D line in sunlight reflected from the surfaces of planets will be doppler-shifted due to both the relative velocity of the planet and the sun and the relative velocity between the vehicle and the planet. This doppler shift is measured by comparing reflected sunlight collected in an optical system to a locally generated sodium line reference. The attainable accuracy of such a velocity-measuring technique, the associated apparatus problems, possible errors due to light emitted as well as other systematic errors, and the necessity for an ephemeris detailing the position and velocity of each of the planets with respect to time are discussed.

C. G. LEHR, I. SILBERMAN, J. W. LOTUS, "Electron Trajectories in a Magnetron," presented at the International Congress on Microwave Tubes, Munich, Germany, June 8, 1960.

Truly "self-consistent" magnetron trajectories have never been obtained before, even for a particular tube under specific operating conditions. The well-known trajectories obtained by Tibbs and Wright during World War II were derived from an assumed space-charge distribution and included only DC and first-harmonic terms in the charge and electric field. This paper presents a continuation of the work of Tibbs and Wright.

In the study described, a new set of electron trajectories were calculated by the use of an IBM 704 computer. The problem was coded in such a way that terms up to the fifth harmonic were included. Five iterations were carried through using Harbree's self-consistent method; convergence to a fixed space-charge distribution, however, was not obtained. The calculations were aided by the development of a new method for improving the initial estimate of the electron field.

J. C. DAVIS, JR., "The *Raysistor*, an Electrical Transformer Using Optical Coupling," presented at the National Convention on Military Electronics, Washington, D.C., June 27, 1960.

The "Raysistor" is a device which utilizes the maximum advances in both light-source and semiconductor art to make a transformer using optical coupling between the input and output circuits. As there is no inductive or conductive coupling between input and output, and since the output approaches a pure resistance, numerous applications are apparent which could not be easily performed by other devices. Applications of the "Raysistor" include the "Rayswitch" for use in telemetery, communications, remote control systems, power supplies, and other control loops where it is desirable to control AC with DC, or where potential differences occur between signal and output circuits.

Comparison is made with present transformer art (a transformer in this case being a device for changing power or information from one form to another); other well known electro-optical devices are discussed; and actual "Raysistor" and "Rayswitch" data are presented.

D. R. FAIRBANKS, M. MARK, "General Considerations for Cooling High Heat Density Microwave Tubes," presented at the Dayton IRE Meeting, Dayton, Ohio, May 4, 1960.

A review of the problem of high density heat transfer in electronic components, including metallic conduction, liquid forced convection with and without local surface boiling, finning, critical temperatures and locations, and evaluation of coolant fluids for forced convection. Typical capabilities and limitations of the various cooling techniques are presented, and specific applications to microwave tubes are discussed. Other factors such as surface roughness, fouling, flow stability with local boiling, and transients are considered.

DIRECT SOLAR POWER CONVERSION

RICHARD C. BARBERA *is Section Head, Space Technology Branch, Advanced Development Department, Missile Systems Division. He has studied infrared and emission spectrographic analysis techniques and has also designed mass spectrometers for the abundance analysis of heavy element isotopes. Since joining Raytheon four years ago he has been active in the design of infrared and optical guidance and detection systems. He is presently studying propulsion and power sources for space systems. He received his B.S. and M.S. degrees in Physics from MIT and Bryn Mawr, respectively.*

DAVID L. DAYTON *is an Engineer in the Space Technology Branch of Missile Systems Division's Advanced Development Department. He obtained his B.S. degree in Electrical Engineering last year from MIT. Since joining Raytheon he has studied ion propulsion systems and the design of experimental facilities for ion engine evaluation.*

ON SOURCES FOR SPACE VEHICLES

THE electrical power requirements of space vehicles have been brought into sharp focus during these first years of the Space Age. In addition to the power needed for communications, navigation, guidance and control, and scientific instrumentation, severe electrical power requirements have been imposed by propulsion systems necessary for the economic exploration of extra-terrestial bodies such as Mars and Venus. (See Electronic Progress, Sept.-Oct. 1959.) Power levels have increased from a few watts to megawatts, and the minimum lifetime of the space power source has increased from a few days to one or two years.

Electrical energy for a space vehicle can be provided in two ways. It can either be drawn out of an energy storage system — such as a battery — or it can be converted from an available source of a different form. Today, there are three major sources of energy: solar, chemical, and nuclear. The utilization of these sources has formed the basis of a new technology, wherein scientists have been forced to re-explore some well known physical processes. The liberation of electrons from a metal or the migration of electrons through a semiconductor, under the influence of solar radiation, was observed a century ago. However, not until the Space Age demanded direct power conversion devices were these phenomena subjected to concentrated investigation.

This article describes only direct solar power conversion devices. In contrast to a solar turbogenerator or a solar regenerative fuel cell, the direct solar power conversion device converts solar energy *directly* into electrical energy. This conversion occurs when a photon exchanges its energy with an electron in a metal or semiconductor, or when the heat of the sun causes thermal emission or thermal migration of the electrons in a metal. The resultant flow of electrons can be utilized to transfer power to a load. At the present time, four direct solar power converters are assuming significance:

The photovoltaic solar cell
The photoemissive converter
The thermionic diode
The thermoelectric generator

Photovoltaic Solar Cell

A photovoltaic cell, consisting of a layer of pure selenium evaporated upon an iron base, generates its own electromotive force when subjected to light. Photons, penetrating the selenium layer, produce photoelectrons at the selenium-iron barrier which are ejected into the selenium. The selenium layer is thereby given a negative charge, and the iron is given a positive charge. The photovoltaic effect has been observed with copper-copper oxide barriers, and also with lead sulphide, silver sulphide, zinc sulphide, and many other elements and compounds when deposited on a suitable base.

The fact that electron flow could be stimulated by sunlight falling on electrodes immersed in an electrolyte was discovered by E. Becquerel over one hundred years ago. In 1876, a similar effect was observed by W. G. Adams and R. E. Day who were investigating the properties of selenium, and in 1884, sensitive selenium barrier-layer cells were prepared by C. E. Fritts.

The practical application of the photovoltaic effect was delayed until 1930 when Lange, a mineralogist, utilized selenium cells in investigations of the light absorption of certain mineralogical specimens. Until

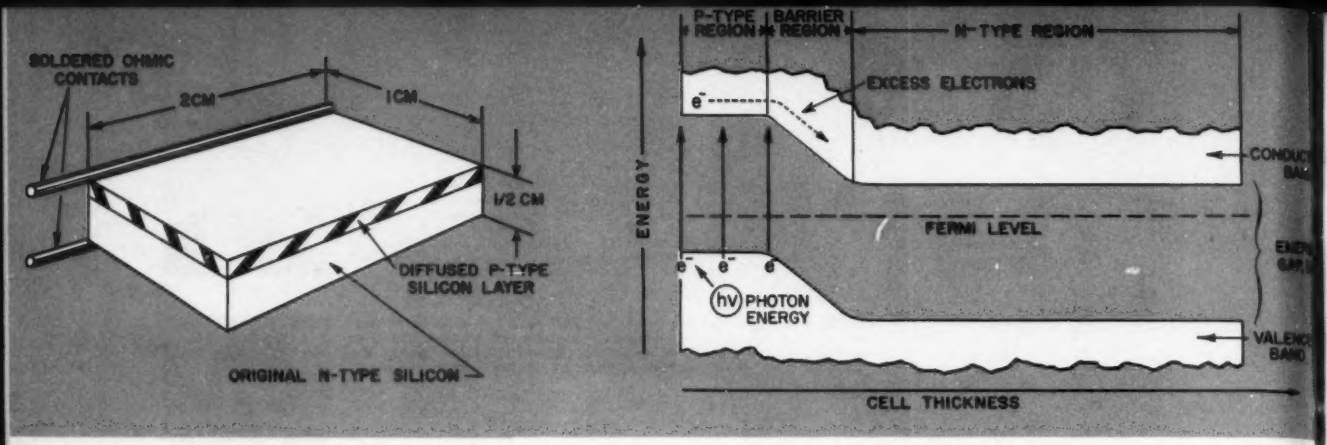

Typical Solar Cell

Figure 1. Energy Level Diagram of Silicon Solar Cell

the early 1950's, the only commercially available photovoltaic device was the Weston Photronic cell — a selenium barrier layer cell used extensively in portable photographic exposure meters. It was not until a requirement for battery charging devices in rural telephone substations was established by the Bell Telephone Company that "solar" cells were reinvestigated.

In 1954, the first practical semiconductor solar cell efficiency was reported. An efficiency of 6 per cent was obtained with a silicon p-n junction. This initial material development has maintained a unique position in the solar cell field; the latest silicon solar cell with a boron diffused junction achieves up to 12 per cent conversion efficiency in production units. No other material has yet been developed which can compete with this device even though, on a theroretical basis, other semiconductors such as gallium arsenide could have a conversion efficiency up to 23 per cent.

Figure 1, the energy level diagram of a silicon solar cell, shows how the conduction and valence bands vary as a function of thickness starting at the converted p-type surface. Under illumination, almost all photons with energy greater than the energy gap, *Eg*, are absorbed within 10^{-5} centimeter of the surface. Each absorbed photon produces an electron-hole pair in the p-type semiconductor which has a high hole density (10^{16} per cu cm) and a low electron density (10^{5} per cu cm). If, under illumination, 10^{12} electron-hole pairs per cubic centimeter are created it is seen that the electron density could be increased by a factor of 10^{7}, while the hole density is only increased by a factor of 10^{-4}. Some of these excess electrons recombine, and others diffuse to the junction and spill over the potential barrier into the n-type semiconductor where they are free to flow into an external circuit and deliver power to the load. However, not all photons in the solar spectrum will be absorbed and produce electrons capable of surmounting the potential barrier. Only a small fraction of the electrons produced possess the required energy and, consequently, the conversion efficiency is a function of the photon energy distribution in the solar source and the response of the solar cell. A typical solar cell response is superimposed on the solar spectrum in Figure 2.

In spite of the relatively low efficiency of 12 per cent, the silicon solar cell possesses characteristics highly desirable as a space power source. A bare solar cell, 2 square centimeters in area, weighs 0.01 ounce. The solar power incident at the orbital radius of the earth is 0.135 watt per square centimeter. Thus, a bare solar cell assembly could deliver about 40 watts of power per pound of weight. In addition to providing a lightweight power source, the solar cell is relatively unaffected by the high energy radiation in space and, with a certain amount of protection, the solar cell power source can have indefinite life under the thermal and mechanical hazards of space. The Vangard I satellite, launched in March 1958, is still obtaining power from its solar cell system. This solar cell package, which is mechanically and thermally protected, could have had a specific power of about 20 watts per pound. However, because of the tumbling of the satellite and the requirement of operation during the dark periods of its orbits, the specific power was much lower than the above figure. Consequently, the satellite was provided with multiple solar cell packages and a battery storage system to compensate for the tumbling and dark periods, establishing the specific power of the complete system at about 3 watts per pound.

Photoemissive Converter

The familiar phototube is a potential solar power conversion device. The action of light falling on a specially prepared metal surface to produce free electrons is analogous to the action of the photovoltaic cell described above.

The photoemissive effect was discovered by Hertz in 1887 as a by-product of his classical researches on electric waves and oscillations. He noted that the ultraviolet radiation of his spark apparatus stimulated electron emission from copper electrodes. However,

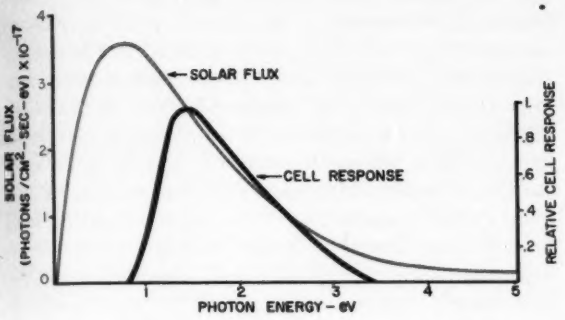

Figure 2. Solar Flux and Response of Silicon Cell

Hertz did not pursue investigation of his discovery. Further precise studies with copper and zinc by Wilhelm Hallwachs in 1888 resulted in photoemission being referred to as the "Hallwachs effect". Numerous investigators were enchanted by this phenomenon and, in 1890, the first true evacuated glass phototube was made by J. Elster and H. Geitel; the photoemissive surface of this phototube was a sodium amalgam. Later experiments by Elster and Geitel, who instinctively recognized the photosensitivity of the alkali metals, resulted in hydrogenated alkali phototubes. These tubes, dating back to 1912, were the forerunners of modern phototubes.

In a metal at any temperature, the electrons which contribute to electrical conductivity possess a spectrum of energies. In order for an electron to escape from the metal, however, it must possess an energy in excess of a certain amount called the work function of the metal. The electrons can acquire this excess energy through elevated temperatures as in a vacuum tube filamentary cathode, or by energy exchange with a photon. During the process of photoemission, the photon energy is transferred to an electron.

Once liberated from the metal, the electrons are available to do work in a load connected between the emitter and the collector. The energy level diagram of the photoemissive process is shown in Figure 3.

Just as in a filamentary cathode, the escaping electrons will contribute to the space charge which surrounds the emitter. This space charge reduces the maximum current flow. Therefore, in the ordinary phototube application, the collector is placed at a positive potential with respect to the emitter in order that all the photoelectrons are collected. However, with a photoemissive solar converter one does not want to supply power to the converter by providing a collecting field. Therefore, the effects of the space charge are reduced by decreasing the spacing between the emitter and collector, or by introducing a source of positively charged particles — as perhaps, a radioactive isotope. Consequently, no accelerating field is supplied to the photoemissive converter, and the electrons working against a retarding field perform useful work in the load.

The photoemissive converter is a *new* solar power conversion device. Experimental investigations of practical converters started about two years ago. The conversion efficiency of this device is a function of the spectral response of the surface, the work functions of the emitter and collector, and the voltage drop across the load. With a cesium antimonide photoemissive surface and a load voltage of 1.3 volts, a solar conversion efficiency of 0.6 per cent can be expected. However, as shown in Figure 4, other materials such as a sodium-potassium-cesium-antimonide alloy offer potentially higher conversion efficiencies, perhaps as high as 2.5 per cent.

As demonstrated in the preceding section, the conversion efficiency of a solar power source is, *per se*, not a measure of its utility in a space application. The more important characteristic is specific power. A typical photoemissive converter for space use would consist of a large area photo-cathode almost touching a collector. This structure might possibly be a 0.005-inch thick plastic sandwich weighing about 0.05 pound per square foot. With a solar conversion efficiency of 2.5 per cent, the specific power of the photoemissive converter would be about 60 watts per pound of weight. This high specific power is obviously desirable and permits the device to be competitive with other sources.

Inasmuch as no photoemissive converters have been constructed and tested in space, one can only speculate on the effects of the environment. Certainly some degree of protection must be provided against ultraviolet and solar X-ray deterioration of the transmission characteristics of the packaging, which might stand a 60°C equilibrium temperature in an Earth orbit quite well. The actual performance of a space photoemissive converter will provide the answers to questions of life, efficiency, and specific power of this new development.

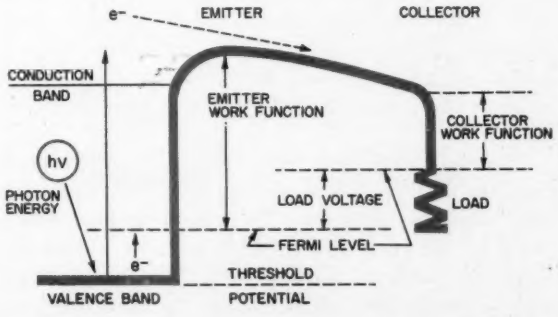

Figure 3. Energy Level Diagram of Photoemissive Converter

Thus far, only power sources which utilize the quantum effects of solar radiation have been discussed. Devices which convert the heat of the sun directly into electrical power are equally important.

Thermionic Diode

The thermionic diode is a unique application of an effect that was known for 200 years — that air in the neighborhood of hot solids has the power of conducting electricity. In spite of these early observations, the emission of electrons from heated filaments was first formulated and studied by Schlichter in 1914. In 1916, O. W. Richardson published an equation establishing a relationship between the electron current density, the temperature, and the work function of the emitter.

The thermionic effect has provided the basis for the development of the vacuum tube, the magnetron, and the many devices that utilize a heated cathode source. However, the exploitation of the combination of a hot cathode emitter and a cooler anode collector as a novel electrical power generator did not occur until 1957. At that time, G. N. Hatsopoulos, in his doctoral dissertation at MIT, investigated the possibility that a thermionic diode might constitute a unique power source.

The conversion process that occurs in a thermionic diode is similar to that which occurs in the photoemissive converter. The only difference between the two devices is that the electrons escape from the cathode because of the high temperature resulting from focused solar radiation. These free electrons then perform useful work in a load. The energy level diagram of Figure 5 illustrates the conversion process, and is similar to Figure 3.

The theoretical efficiency of the thermionic diode is equal to the ratio of power delivered to the load to the power input to the cathode. This efficiency is a function of the load voltage, work functions of the cathode and anode, and the temperatures. Since the thermionic diode is a heat engine in a thermodynamic sense, its efficiency will be limited by the efficiency of a Carnot cycle. Thus, theoretical efficiencies of the order of 45 per cent are possible for a thermionic diode operating between 1375°K and 2500°K. Experimental engines have been tested in this temperature range, and efficiencies of 13 per cent have been obtained.

The efficiency losses in a thermionic diode arise from the effects of space charge, anode emission, and heat losses by radiation. The retarding field established by the space-charge cloud tends to reduce the maximum electron current flow. This, by analogy with a conventional heat engine, reduces the heat transfer between the source and the sink. Two obvious techniques for decreasing the effects of space charges involve the use of close spacings (0.0005 inch) between the elements, or the use of positive ions as obtained from cesium vapor introduced in the device. These techniques, also useful in the photoemissive converter, are somewhat effective in this application. However, the close spacing of the elements introduces the problems of anode emission and cathode heat radiation losses, which are under intensive investigation at the present time. The applications of heat transfer and electron physics techniques will aid in the attainment of high efficiency thermionic diodes.

Although experimental models of a thermionic diode converter have been no larger than 1 square centimeter in area, the device is not limited in size. A space solar power source application would require a cathode area several hundred times this size and a much larger solar collector in order to provide reasonable power levels. The low temperature of the converter is achieved by the use of a radiator. This combination of the solar collector and radiator adds considerable weight to the conversion systems so that the maximum specific power of the system may be about 12 watts per pound. This reasonable specific power, in addition to potentially long life, allows the thermionic diode to assume a favorable position as a direct solar power source for space use.

Thermoelectric Generator

The thermoelectric generator is a unique application of an old device — the thermocouple. Ever since Seebeck discovered the thermoelectric effect in 1821, experimenters have been investigating the electrical phenomena associated with establishing a thermal gradient across metals. There is not a student of physics who has not fashioned many thermocouples of combinations of metals, such as copper and constantan or iron and constantan. Yet the thermoelectric effect

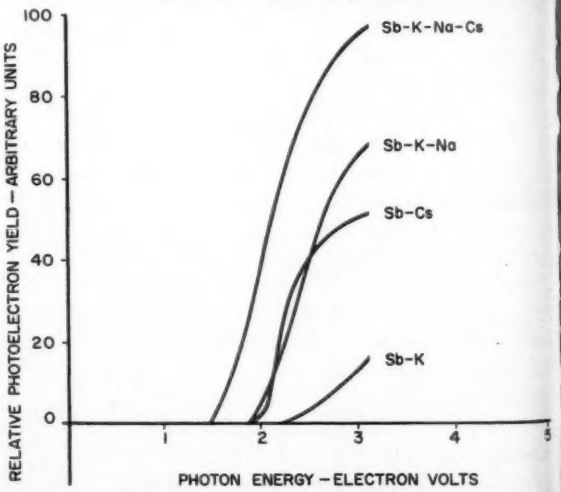

Figure 4. Response of Various Photoemissive Cathodes

has not been limited to the accurate measurement of temperature. In the 1930's, the Russians developed thermoelectric generators out of necessity for electrical power in rural areas. These small portable devices, flame-heated and intended for home use, are still effective. At about the same time, Dr. S. Kanar of the Baltimore Gas and Electric Company initiated the development of the thermoelectric converter for control valve activation in home gas furnaces and hot water heaters. These control valves are widely used today.

The simplest form of a thermoelectric generator, illustrated in Figure 6, consists of two semiconductors — one p-type and one n-type. Just as in the ordinary thermocouple, a temperature difference between the hot and cold junctions produces a voltage which is proportional to the temperature difference. This voltage can be used to drive electrons through an external load.

The effectiveness of a thermoelectric generator is measured by a figure of merit defined as:

$$Z = \frac{a^2}{K\rho},$$

where a is the thermoelectric voltage produced per degree temperature difference, K is the thermal conductivity of the combination, and ρ is the electrical resistivity of the generator. Obviously, this figure of merit is nothing more than a statement of the fact that a good thermoelectric generator must be capable of maintaining a temperature difference between the hot and cold junctions, and must be a high power conversion source with low impedance. Unfortunately, this figure of merit is a decreasing function of temperature, and the thermoelectric generator is confined to operation at lower temperatures than the thermionic diode in order to attain reasonable efficiencies.

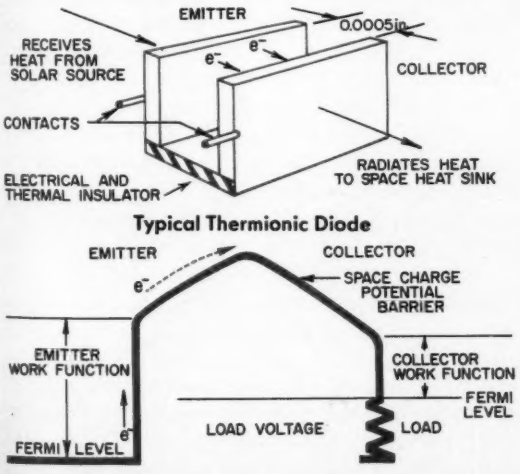

Figure 5. Energy Level Diagram of Thermionic Diode

A practical thermoelectric generator would have a figure of merit of 3×10^{-3} per degree. A thermoelectric generator fabricated from bismuth telluride and lead telluride would have a maximum conversion efficiency of 8.2 per cent of Carnot cycle efficiency when operating between 600°K and 300°K. It is anticipated that research and development will provide materials capable of operating at higher temperatures, thereby making it possible to achieve up to 12 per cent Carnot cycle efficiency.

In its present state of development, the thermoelectric generator is somewhat disappointing. Although the lifetime of the device is unlimited, the specific power of a space solar conversion system would be about 1 watt per pound. This is much lower than the specific powers of the direct converters previously described. However, the thermoelectric generator possesses advantages when coupled with the thermionic diode converter. In a hypothetical configuration, the thermoelectric generator could act as a heat sink for the thermionic diode; such cascading could provide a solar power source with a specific power higher than both combined because of the reduced requirements for a heat radiator for the thermionic diode. Configurations such as these are being given serious consideration at the present time.

These direct solar conversion devices are applications of discoveries which were made long before the requirements of space power were established. Solar devices, which now appear so unique, could perhaps have been developed more than 50 years ago. If Hertz or Bequerel had pursued their discoveries with the vision of utilizing solar power for man's eventual use, and if Richardson, Seebeck, and those who followed had felt the need for an abundant energy source for conversion to electrical power — what type of power source would we be using today?

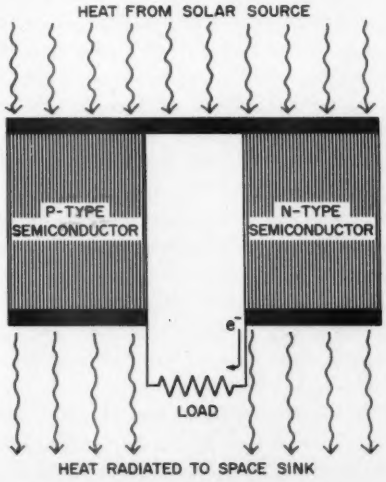

Figure 6. Thermoelectric Generator

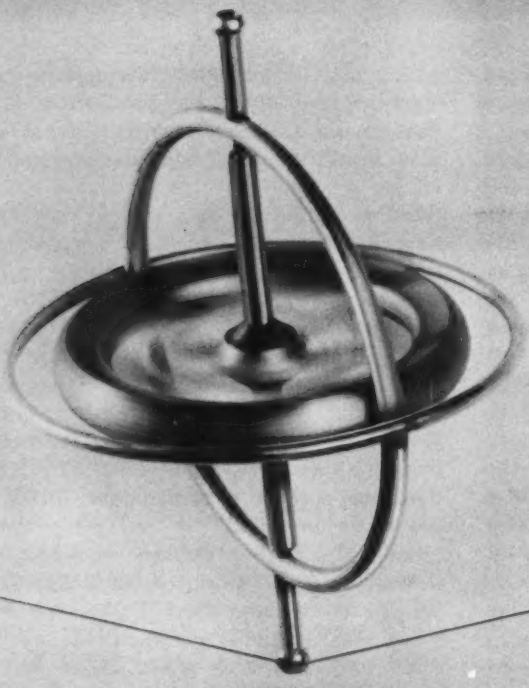

sta

STABILIZATION has almost as many meanings as there are people to define the term. To the systems engineer, stabilization refers to the process of ensuring that a certain class of systems such as servomechanisms, regulators, and computers is not self-oscillatory. To the banker or the economist, stabilization refers to the process of smoothing the effect of normal or abnormal economic cycles. Yet, despite any apparent differences, the stabilization processes in these examples are actually the same. For the purpose of this article, stabilization will be considered a form of isolation or separation of phenomena for the purpose of improving some performance index. As an example, consider the process of maintaining body temperature against changes in local environmental conditions. Man has provided himself with clothing of different weights, light for summer and heavy for winter, and has a central heating plant in his home which he controls with a thermostat. In many instances, he has an external thermometer equipped with a differentiator to sense the rate of temperature change outside the house. By controlling the rate of heat transfer between himself and his environment, he isolates or separates his own internal body chemistry from the external phenomena which affect his body temperature. Thus he improves his comfort and consequently his effectiveness.

There are only two fundamental approaches available for the solution of any stabilization problem, although there are many ways of implementing either approach. To illustrate one approach, consider the problem of minimizing or eliminating from the output of a direct coupled amplifier the drift due to temperature changes. The most widely used method (until recent years) is shown in Figure 1a. Here a basic amplifier is tested to determine the drift signal, e_d, as a function of temperature. Then a compensator is designed to produce a compensating signal, e_c, equal but opposite to e_d. Depending upon the success of matching e_c and e_d, the output, e_o, is either totally or partially corrected for temperature. This approach is popularly called temperature compensation.

The alternate approach to the drift problem would be the use of a chopper-stabilized amplifier as shown in Figure 1b. The bandwidth of the chopper amplifier is usually quite small (a few cycles per second), since its only function is to reduce the effect of any internally generated and unwanted voltage, such as drift. It can be shown that any internally generated signal is effectively decreased by approximately the gain, k, of the chopper amplifier, while the normal input signal, e_i, proceeds through the basic amplifier uninhibited.

There are important similarities and differences between the two approaches. Both approaches use a means of measuring or sensing, and both apply corrective action. They differ in *what* is measured or sensed, and *when* the corrective action is applied. In the temperature compensation example, it is the *temperature* which is measured. This is done by the compensator, which may be a thermistor (a temperature sensitive resistor). The compensation signal, e_c, may

ilization

RICHARD E. LANG *is a Senior Engineer, Ordnance Radar Dept., Wayland Laboratory. He has had varied experience in both industry and education in mechanical design, dynamic analysis, and automatic control. Now in his fifth year at Raytheon, he is a group leader responsible for analysis, design, and development of servomechanisms primarily for military radar systems. Mr. Lang holds B.S., M.S., and M.E. degrees from MIT.*

appear at the output either earlier, simultaneously, or later than the drift signal, e_d, depending upon the thermal delay of both the amplifier and compensator. Furthermore e_c may be exactly equal and opposite to e_d, resulting in total compensation. In addition, the chain of events proceeds unidirectionally, and never folds back upon itself. Processes with this characteristic are termed open-loop systems.

In the second example, the *actual drift signal* appearing in the output is measured. This is accomplished by the feedback loop. The corrective action taken by the chopper amplifier always appears later than the original drift signal, e_d. Furthermore, the cancellation can never be complete or total, but can come as close to complete as practical limits will permit. It should be noticed that the chain of events folds back upon itself forming a closed loop. Processes with this characteristic are known as closed-loop or feedback systems.

Each of these two fundamental approaches, open-loop and closed-loop, has advantages and disadvantages. The following detailed example of stabilization of coordinate tracking systems illustrates the application of these basic approaches to a specific problem, and discusses one of the numerous stabilization problems associated with this class of systems.

Coordinate Tracking Systems

The primary function of coordinate tracking systems is to follow a target in space to derive information concerning the relative position between the tracker and the target. Coordinate tracking systems include the inertial navigator which may track a local gravity vector for the purpose of navigating, the 200-inch telescope at Mount Palomar which may track celestial bodies such as the sun to photograph solar activity, and the radar on an instrumentation ship which may track a missile to determine its trajectory. Although in these situations the objects tracked and the reasons for tracking are all different, the primary data are identical — space coordinates.

This example describes mechanical tracking systems only, since electrical or optical trackers using multiple beams can be shown to be equivalent to mechanical systems, the major difference being the inertia and speed of response of the moving members.

Because tracking systems have finite size and mass, they are supported on a base which may be part of or attached to the earth, the deck of a naval vessel, or the frame of an aircraft or satellite. The orientation of the base and the direction from which the target may appear are generally random functions, hence, it is necessary to be capable of moving the tracker about a minimum of two axes, usually orthogonal. This will permit the tracker to see the target for any orientation within the physical limits of design. (There are positions during which the base will eclipse the target.) A typical two-axis configuration is shown in Figure 2.

Since the minimum number of axes is two, one might well ask, "Why are there ever more than two?"

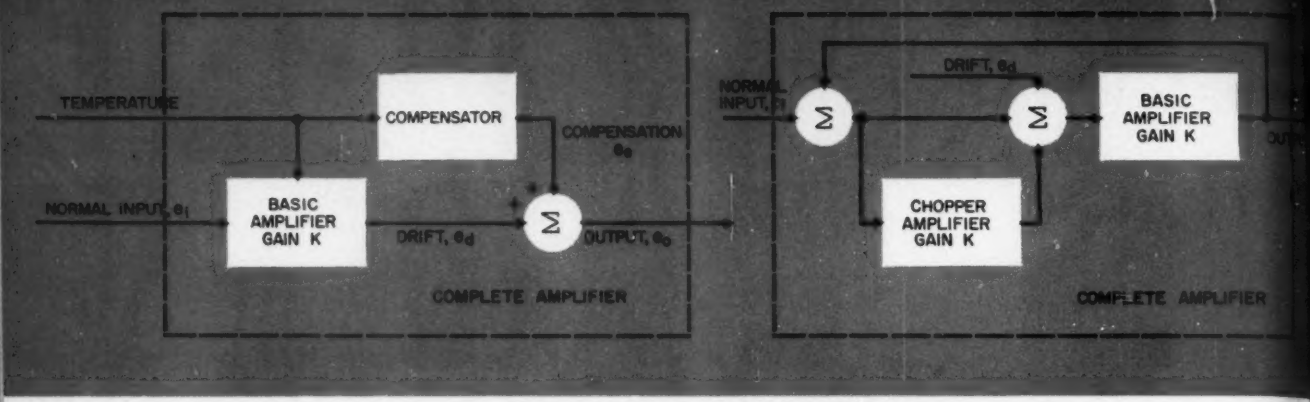

Figure 1. Two Approaches to Stabilization

There are only two major reasons for providing three or more axes. The first involves the six degrees of freedom possessed by both the base and the target, three translational and three rotational, as shown in Figure 3. In most cases, the angular orientation of the target about its own center of gravity is unimportant. The target rarely subtends an angle large enough to permit resolution and measurement of this motion, and is usually considered a point with translational motion only. Quite conveniently, the tracking system measures relative motion between the base and the target making it possible to lump the translational motion of the base with that of the target. The only motions unaccounted for are the three angular motions of the base; a two-axis mount can accommodate two of these. The third motion unaccounted for appears as a rotation about the line of sight (LOS) and is called cross-roll.

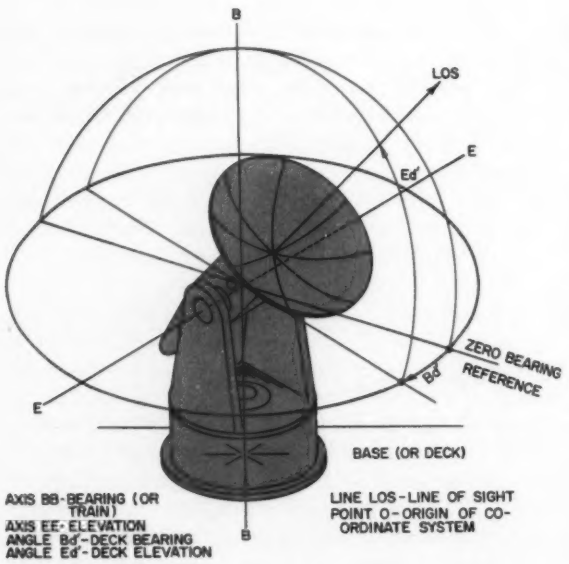

Figure 2. Typical Two-Axis Tracking System

This rotation about the LOS may be illustrated by assuming we are in a submarine with the periscope just at water level, and the target is dead ahead. While the submarine is horizontal, movement about the bearing axis BB (Figure 4) scans the target from left to right, and movement about the elevation axis EE scans the target from top to bottom. As the submarine rolls, the target remains in the cross-hairs but is rotated with respect to the bearing and elevation axes. No combination of movement about the two axes will permit us simultaneously to see the target and to align the axes vertically and horizontally as they were before the submarine rolled. Therefore, the additional axis is used to accommodate for cross-roll, and might also be used in radar, radio, or optical communication links where information is polarized. The most convenient orientation for this axis is parallel to the LOS, thus permitting the reflector of Figure 2 to be rotated about the LOS as though it were being screwed into or out of the mount.

The second reason for using additional axes is to minimize or eliminate certain physical limitations, particularly the inability of anything to achieve infinite or near infinite speed and power. The most frequent occurrence of this limitation arises when the target passes near the extension of the first axis from the base. In Figure 2, this is the bearing axis, and the target is nearly over head. The angular rate of the mount about the bearing axis needed to keep the LOS on the target is given by: $DB_d' = \omega_T \, Sec \, E_d'$, where D = time derivative (d/dt), and ω_T = angular rate of target. It can be seen from this equation that DB_d' approaches infinity for any finite target speed as the elevation angle, E_d', approaches 90°. The ratio DB_d'/ω_T, shown in Figure 5, is moderate from 0° to 60° elevation but increases rather rapidly from then on. Current practice is to limit this ratio between 6 and 10, corresponding to 80° to 85° elevation. This means that within a 5° to 10° cone about the first axis there is no guarantee that the target can be tracked. When this is combined with possible deck or base motion as shown in Figure 6, the results are staggering. Typical values for deck motions of naval vessels

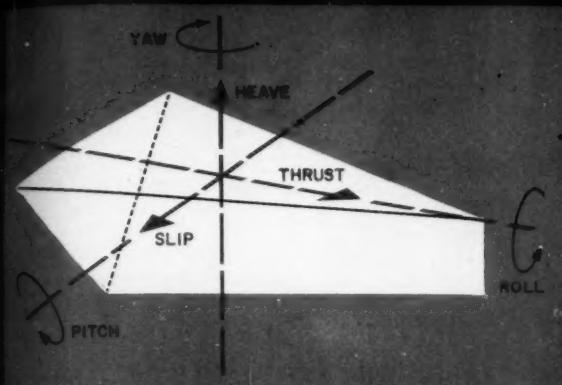

Figure 3. Six Degrees of Freedom of a Rigid Body

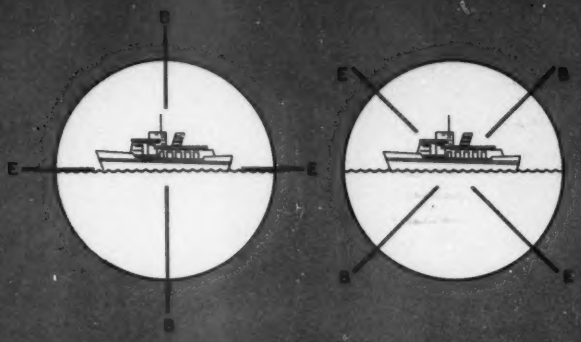

Figure 4. Rotation about the LOS — Cross Roll

are ±5° pitch and ±30° roll. There are additional factors which tend to increase the size of the blind zone. Luckily, there is almost zero probability that a target will be going at maximum speed and minimum range within the blind zone while the deck has undergone its maximum excursion. If, however, one of the requirements of the tracking system is that no blind zone shall exist due to limitations of maximum speed or power capabilities, then an additional axis is necessary.

The usual axis employed in this case is the traverse axis shown in Figure 7; the reflector has been omitted to prevent obscuring the detail of the traverse axis. This axis is selected because the amount of material to be moved decreases as the axes get closer to the LOS; the converse is true as the axes recede from the LOS. Ideally the traverse axis does not require a greater angular rate than the target. While the target is in the bearing axis blind zone, tracking is actually accomplished with the traverse and elevation axes. This permits the bearing axis to lumber around and catch up to the target after leaving the blind zone. Outside the blind zone, bearing and elevation accomplish tracking, and traverse goes along for the ride.

In general, tracking systems of more than two axes are the exception, rather than the rule. The inclusion of one or more additional axes adds expense and complexity which are only justifiable when system requirements cannot be met otherwise. Since the axes about which the tracking mount rotates are attached to and rotate with the base, it is apparent the base angular motion disturbs the LOS. The following discussion on velocities induced by base motion and their isolation will be limited to the two-axis configuration of Figure 2. The extension of the principles involved to configurations with more than two axes is largely one of geometry.

Induced Velocity

The angular motions of the deck (or base) are defined as yaw, pitch, and roll, a system of nomenclature which is generally used in discussions of coordinate tracking systems. However, since the pertinent angular rates are components of from one to three separate vectors, certain liberties will be taken in an effort to shorten otherwise lengthy mathematical statements. Let us, therefore, define the instantaneous deck rates as: level rate, ω_1, yaw rate, ω_2, and cross level rate, ω_3, as shown in Figure 8. These instantaneous rates represent an orthogonal coordinate system oriented to the LOS. The level rate, ω_1, is the angular rate of the deck about the elevation axis. The yaw rate, ω_2, is the angular rate of the deck about the bearing axis. The cross level rate, ω_3, is the remaining component of deck motion and is normal to both bearing and elevation axes. Rates ω_1 and ω_3 are contained in the deck while ω_2 is normal to the deck. The total deck rate, ω_d, is the vector sum of ω_1, ω_2, and ω_3.

As the deck rotates, it tends to move the LOS with it inducing a velocity, V_d, at the tip of the unit vector along the LOS. The relationship is

$$\vec{V}_d = \vec{\omega}_d \times \vec{1}. \qquad (1)$$

The LOS is stabilized when some instrumentation process forces the mount to have angular rates which cancel V_d. Denoting the vector sum of DB_d' and DE_d' as ω_m, the velocity, V_m, produced by mount motion is given by

$$\vec{V}_m = \vec{\omega}_m \times \vec{1}. \qquad (2)$$

Thus stabilization is accomplished when

$$\vec{V}_m = -\vec{V}_d. \qquad (3)$$

Base Motion Isolation

In order to evaluate the effectiveness of base-motion isolation techniques, consider the single axis (bearing) of a conventionally stabilized radar tracking loop in Figure 9. The primary reference element is the gyro which is essentially an inertial tachometer. The conventional tachometer measures the relative angular velocity between its stator and rotor. The gyro, on the other hand, measures the relative angular velocity

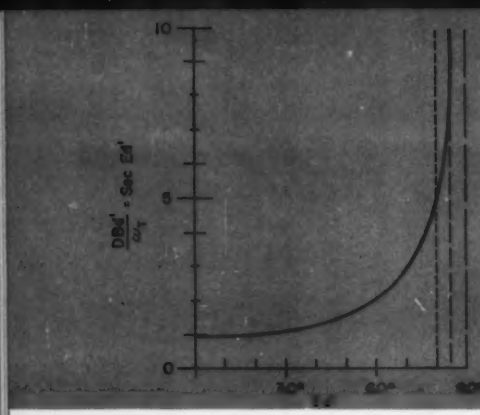

Figure 5. Ratio of $\frac{DB_d'}{\omega_T}$

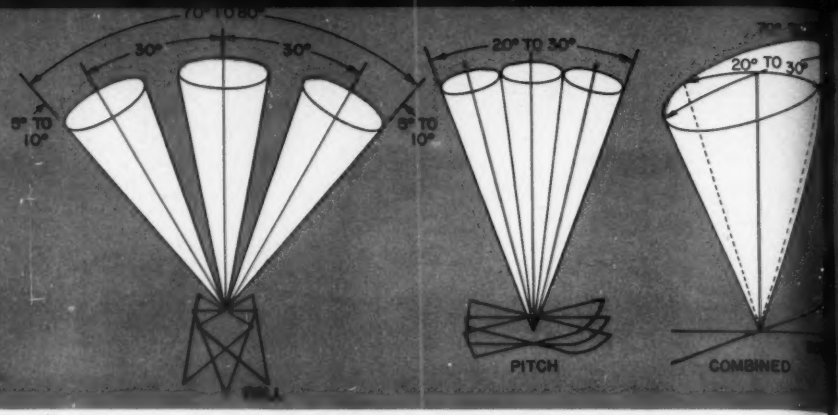

Figure 6. Blind Zone Created by Base Motion and Velocity Illumination

between itself (or the element to which it is mounted) and a coordinate system which is fixed in space.

The system of Figure 9 is considered weakly stabilized because both stabilizing and tracking loops have a common path, the gyro. The LOS must be disturbed for the stabilizing loop to function. This is the same closed-loop process as that used in the chopper-stabilized amplifier.

The $\cos E_d'$ term in the block diagram of Figure 9 is a geometrical quantity. The power drive moves the mount about the bearing axis, whereas the gyro is placed in the LOS and measures angular rate DB_{sd} about the traverse axis. To remove the E_d' dependency from the stabilization loop, a secant correction ($\sec E_d' \cos E_d' = 1$) is added. The gyro loop gain, K_g, and position loop gain, K_p, are, in general, functions of the Laplace operator "s". The signal flow paths represented by solid and broken lines are electrical and mechanical paths, respectively.

The disturbance to the LOS rate and angle caused by base motion is

$$DB_{sd} = \frac{-s\,(\omega_2 \cos E_d + \omega_3 \sin E_d')}{s\,(K_g + 1) + K_g K_p}, \qquad (4)$$

and

$$B_{sd} = \frac{-(\omega_2 \cos E_d' + \omega_3 \sin E_d')}{s\,(K_g + 1) + K_g K_p}. \qquad (5)$$

Since tracking loop requirements and base motion characteristics differ widely from application to application, a quantitative analysis is restricted in value. Qualitatively, however, the disturbances of Equations 4 and 5 are reduced as K_g and K_p are increased. Stability of closed-loop systems places an upper bound on the maximum usable K_g and K_p, thus limiting the minimum value of Equations 4 and 5.

In applications where the maximum loop gains of Figure 9 do not permit sufficient isolation, the strongly stabilized tracking loop of Figure 10 may be used. It differs from the technique previously discussed by the inclusion of a tachometer loop with gain K_t and gyros, tangent pot, and filter to measure and shape base motion rates prior to summation with tachometer feedback. It is termed strongly stabilized since the stabilizing and tracking loops do not necessarily have common paths. Indeed if the filter, F, has the transfer function

$$F = \frac{K_t + 1}{K_t}, \qquad (6)$$

then

$$DB_d' - (\omega_2 + \omega_3 \tan E_d') = 0.$$

Thus the LOS is totally stabilized without being disturbed.

In practice it may be difficult or even impossible to satisfy Equation 6 over the entire frequency range. This is not serious. Excluding external influences which would produce catastrophic effects, the base usually presents a high-Q impedance to the disturbing forces, therefore restricting base motion to a narrow band of frequencies. Taking advantage of this fact, a filter can be designed to satisfy Equation 6 as closely as desired over the frequency range of interest.

The approach shown in Figure 10 is a combination of both open- and closed-loop approaches, and contains the advantages of both without the disadvantages of either. If the measurement of base motions ω_2 and ω_3, and the computations of the input signal and the mount response are exact, stabilization is complete with no base motion appearing on the LOS. However, if the process is correct to 10 per cent, then approximately 10 per cent of base motion appears on the LOS for the tracking loop gyro to remove. This is an order of magnitude improvement over the conventional method which uses no measurement of base motion and no computation of inputs.

The extension of the block diagram of Figure 10 to include the elevation axis requires only expansion of the vector relationships of Equations 1, 2, and 3 to determine the necessary conditions to be satisfied.

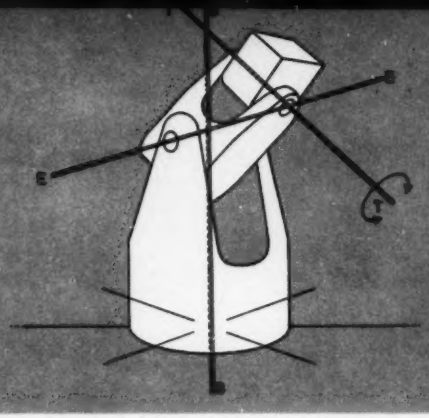

Figure 7. Three-Axis System

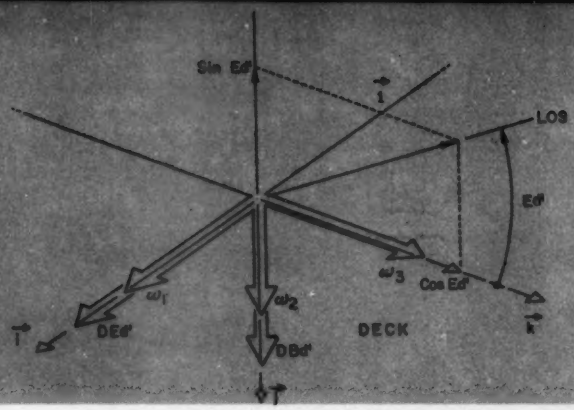

Figure 8. LOS Oriented Coordinate System

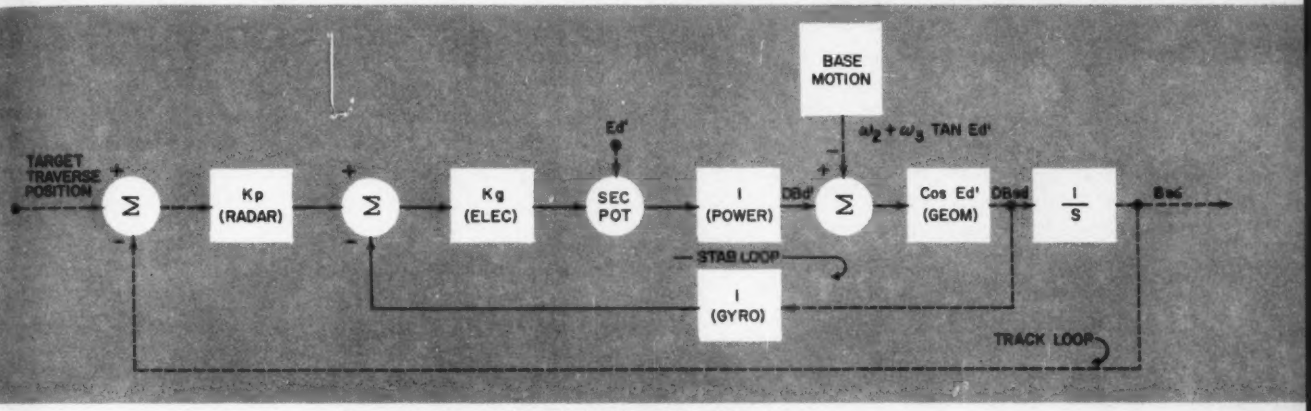

Figure 9. Conventionally Stabilized Tracking Loop

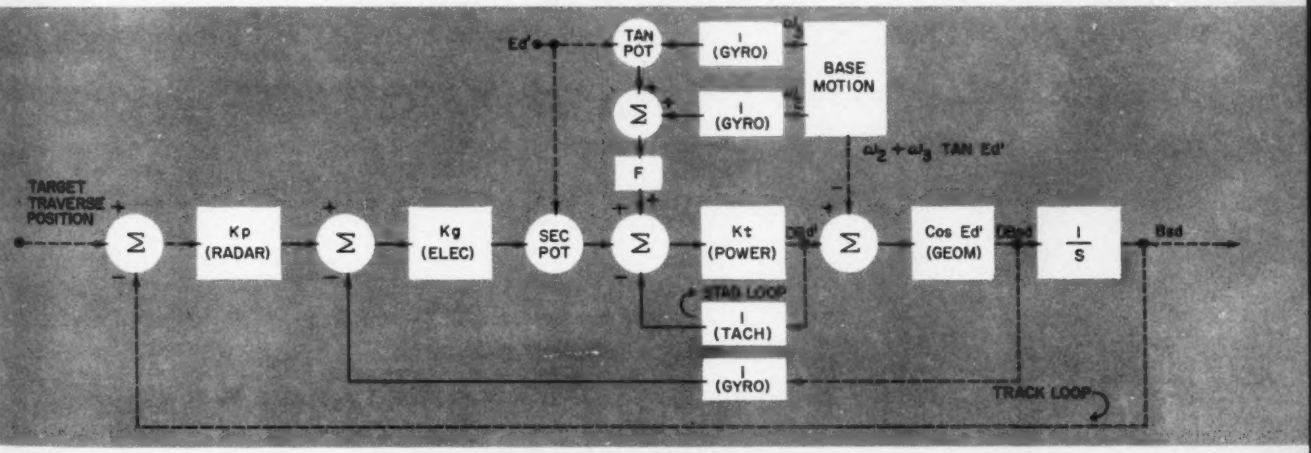

Figure 10. Strongly Stabilized Tracking Loop

INVENTIONS

Congratulations to the following persons for their valuable contribution to Raytheon's portfolio of inventions:

Name	*Field of Invention*
A. J. Aronian, A. H. Moore	Automatic Shutoff
Ashod S. Dostoomian	Capped Cathode
Pascal Levesque	Mold Assemblies for Fabrication of Semiconductor Devices
Benjamin D. Roiter, Bennett Bovarnick, Seymour L. Blum, David A. Belforti	Pyrolytic Boron Nitride and Method of Producing Same
Herbert S. Sobel	Magnetic Shift Registers
Ralph Lanciano	Induced Electrophoresis
Irving Goldstein	Traveling Wave Parametric Amplifier
David L. Bobroff	Degenerate Parametric Amplifier with Idler Cancellation
Wilfred G. Beauregard	UHF High Power Isolator
Ernst Schloemann	Ferrite Resonance Isolators
Gordon R. Partridge	Fault Location
Costas E. Goltsos	Weight Reduction Technique

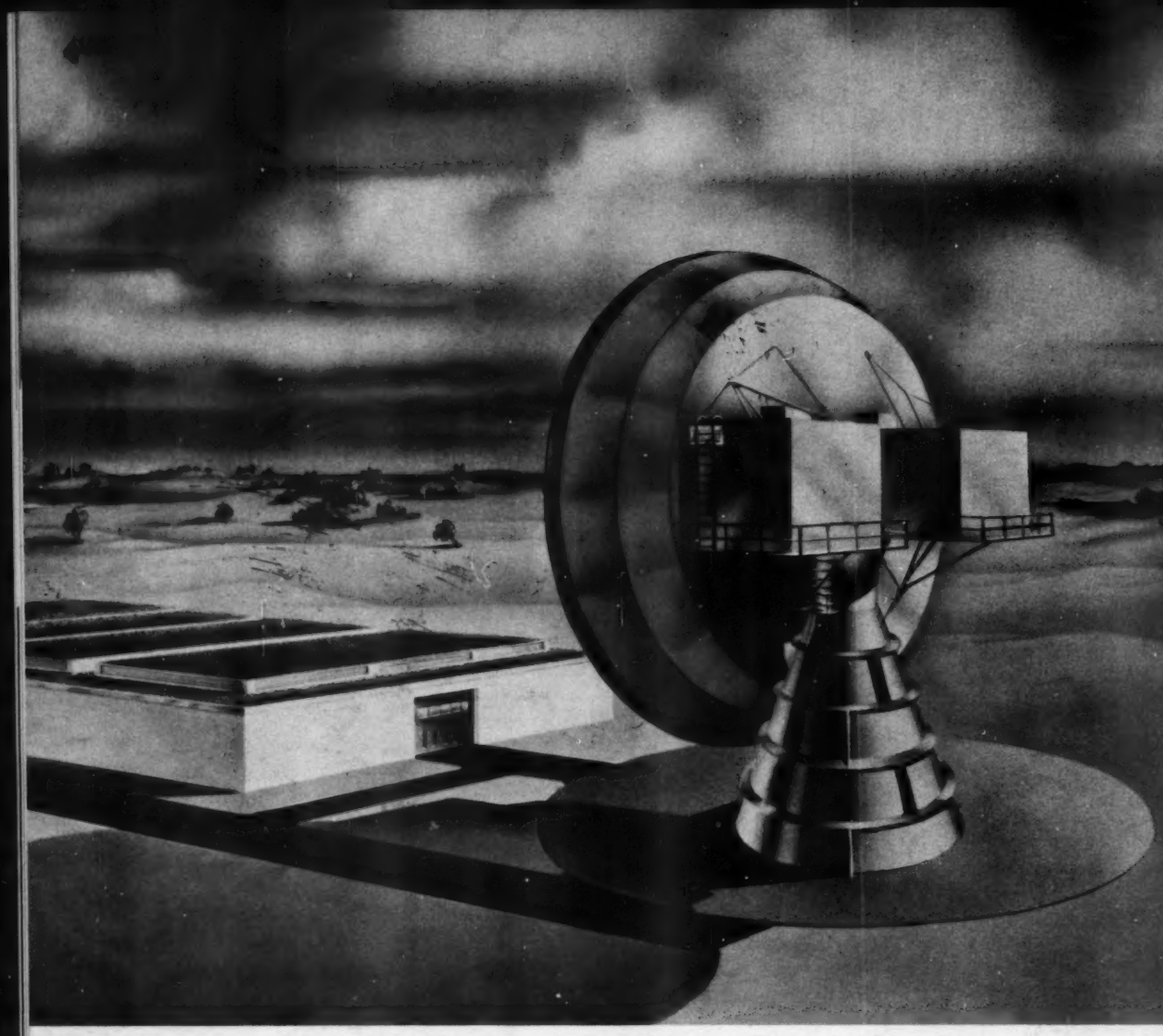

Five-story high antenna for Pincushion radar will be part of a new Advanced Research Projects Agency installation to be set up in mid-Pacific.

A unique radar designed to track and identify the warhead of ICBMs thousands of miles away is now being developed by Raytheon.

Designated "Pincushion", because of its microwave beam pattern formation, the 80-ton Raytheon radar will be part of Project Defender, ARPA's program to develop advanced anti-ICBM concepts.

RAYTHEON COMPANY, WALTHAM, MASS.

RAYTHEON

EXCELLENCE IN ELECTRONICS